A Full Analysis Note on the Measurement of the Branching Fraction of D_s Inclusive Semileptonic Decay $D_s^+ \to e^+X$

(November 23, 1996)

Abstract

The absolute inclusive semileptonic branching fraction of $D_s^+ \to e^+X$ has been measured based on 22.3 pb^{-1} e^+e^- collision data collected with BES at $\sqrt{s} = 4.03$ GeV/c^2. At this enery, D_s are produced in pairs: $e^+e^- \to D_s^+D_s^-$. We reconstructed D_s decay events in five hadronic decay modes. In the recoil system of these events, several D_s inclusive semileptonic decays were observed, and the branching fraction was estimated by two different methods.

I. INTRODUCTION

The spectator model predicts equal lifetimes for D^+, D^0, and D_s. This prediction is incorrect; the D^+ lifetime is about twice as long as that of the D^0 and the D_s [1]. The inequality is believed to be due to final state interference in hadronic D^+ decays; the semileptonic decay widths are still expected to be approximately equal, *i.e.*, $\Gamma_{SL}(D^+) \approx \Gamma_{SL}(D^0) \approx \Gamma_{SL}(D_s)$. MARK-III measured the inclusive semileptonic branching fraction of D^+ and D^0 produced in decays of the ψ'' resonance [2]. Their results, $B(D^+ \to e^+X) = 17.0 \pm 1.9 \pm 0.7\%$ and $B(D^0 \to e^+X) = 7.5 \pm 1.1 \pm 0.4\%$, are consistent with $\Gamma_{SL}(D^+) \approx \Gamma_{SL}(D^0)$ considering the difference in lifetimes. If this relation extends to the D_s, then $B(D_s^+ \to e^+X)$ should be about 8%. This branching fraction was measured by MARK-III at $\sqrt{s} = 4.14$ GeV/c^2 with a fairly large error, resulting in an upper limit of 20% at 90% C.L. [3].

This paper reports a new measurement of the inclusive D_s semileptonic branching fraction with data collected with the Bejing Spectrometer (BES) [4] at $\sqrt{s} = 4.03$ GeV/c^2, just above the $e^+e^- \to D_s\bar{D}_s$ threshold. We detect one of the two D_s via its hadronic decay into $\phi\pi^+$, $K^{*0}K^+$, $K_S^0K^+$, $K_S^0K^-\pi^+\pi^+$, or $f_0\pi^+$ and search the recoil system for semileptonic decays with one well identified electron track. Charge conjugate decay modes are implicitly assumed throughout this paper.

II. D_S SINGLE TAG

At $\sqrt{s} = 4.03$ GeV/c^2, D_s mesons can only be produced via $e^+e^- \to D_s^+D_s^-$. The total energy of a D_s candidate must be equal to the beam energy $E_{beam} = 2.015$ GeV/c^2. Hence, the beam-constraint can be imposed on the measured momenta of D_s daughter particles via a kinematic fit (a 1-C fit) to improve the measured D_s mass resolution. This constraint is applied in the analysis presented here.

The D_s mesons are reconstructed in five hadronic decay modes: $\phi\pi^+$, $K^{*0}K^+$, $K_S^0K^+$, $f_0\pi^+$, and $K_S^0K^-\pi^+\pi^+$, with subresonances decaying as $\phi \to K^+K^-$, $K^{*0} \to K^-\pi^+$,

$K_S^0 \to \pi^+\pi^-$, and $f_0 \to \pi^+\pi^-$. Events are selected which contain at least three reconstructed charged tracks. The error matrix of each track is corrected by the subroutine ERMXCR which is in the BES code library; the momentum scaling caused by the magnetic field problem is considered in V87 TELESIS code WAITER. In order to ensure good momentum resolution, all tracks used in the single tag are required to have a good helix fit (MFIT=2,-19) in the main drift chamber with a fiducial cut $|\cos\theta| < 0.8$, and to originate from the production vertex ($r < 2$ cm and $|z| < 20$ cm). Pions consistent with K_S^0 decays are exempt from the vertex cut. Pions and kaons are identified by a combined confidence level of TOF and dE/dx measurements. Identification requires consistency with the pion or kaon hypothesis with a confidence level greater than 0.1%. In order to reduce misidentifications, all kaon candidates are further required to have a larger confidence level for the kaon hypothesis than for pion hypothesis except for $K_S^0K^+$ tagging mode. And in order to suppress the background, all pion candidates are required to have a larger confidence level for the pion hypothesis than for kaon hypothesis in $f_0\pi^+$ tagging mode.

Possible track combinations for each final state of the five D_s decay mode are subject to the 1-C kinematic fit; events with a probability $P(\chi^2) > 10\%$ are kept for further analysis. A requirement on the difference between the measured energy of the D_s candidate and the beam energy, E_{diff}, effectively suppresses the background from D decay. The $|E_{diff}| <$ 50 MeV is required in all modes except $K_S^0K^+$, where an asymmetric cut -50 MeV $<$ $E_{diff} < 20$ MeV is imposed instead, because the kaon identification is poorer and meanwhile E_{diff} distribution of D background is centered at the positive side in this mode. A mass cut on the subresonances $\phi, \bar{K}^{*0}, K_S^0$, and$f_0$ further suppresses the background. We require $|M(K^+K^-) - M(\phi)| < 18$ MeV$/c^2$, $|M(K^-\pi^+) - M(\bar{K}^{*0})| < 50$ MeV$/c^2$, $|M(\pi^+\pi^-) - M(K_S^0)| < 22$ MeV$/c^2$ and $|M(\pi^+\pi^-) - M(f_0)(980MeV/c^2)| < 30$ MeV$/c^2$. The polar angle, θ_h, in the $\bar{K}^{*0}$ helicity frame is restricted by $|\cos\theta_h| > 0.35$ to reduce background in the $\bar{K}^{*0}K^+$ mode. For the K_S^0 reconstruction, we require the momentum vector of the two oppositely charged pions to be aligned with the position vector of the secondary vertex in the xy plane with a confidence level greater than 10%. The secondary vertex is required to be at least 5 mm (in $K_S^0K^+$ mode) or 1.5 mm (in $K_S^0K^-\pi^+\pi^+$ mode) away from the production vertex, and the z coordinates of the two pion tracks to be within 4 cm of the secondary vertex, in order to reduce mis-matching pion pairs. The D_s production angle relative to beam direction is required to be $|cos(\theta)| < 0.6$ in $f_0\pi^+$ tagging mode.

After the above cuts, D_s signals are clearly seen in the mass spectra (see Figure 1). The peak beside D_s in $K_S^0K^+$ mode (Figure 1(c)), and hence the combined spectrum (Figure 1(f)), are due to $D^+ \to K_S^0\pi^+$ produced via $e^+e^- \to DD^*$, where the pion is misidentified as a kaon. The peak can be reproduced by DD^* Monte Carlo simulations. Fitting the mass spectra with one/two Gaussian plus a second order polynomial background yields the number of tagged events for each of the five decay modes as well as the total number of single tags, $171 \pm 21 \pm 15$ with the D_s peak at 1969.0 ± 0.6 MeV$/c^2$ with a resolution of 4.2 ± 0.5 MeV$/c^2$ for five tagging modes; and $147 \pm 19 \pm 13$ with the D_s peak at 1968.7 ± 0.6MeV$/c^2$ with a resolution of 3.9 ± 0.6MeV$/c^2$ for four tagging modes without $D_s \to f_0\pi^+$. In the fit signal number, the first number is statistical error; the second number is systematic error obtained by varying the parametrization of the background.

A. $K^{*0}K^+$ tagging mode checking

In K_S^0K mode, the efficiency will be reduced greatly if the K candidate track is required to have greater probability for kaon hypothesis than that for π hypothesis. The primary K in $K^{*0}K^+$ mode is similar to the K in $K_S^0K^+$ mode. What is the efficiency loss for $K^{*0}K^+$ mode?

Figure 2(a) is the single tag of $D_S \to K^{*0}K^+$ mass plot by requring the kaon probability be greater than 1% for the two K candidate tracks. Figure 2(b) is the result by further requiring the low momentum kaon candidate track has greater kaon hypothsis probability than π hypothesis probability. Figure 2(c) is the result by requiring both K candidate tracks have greater kaon hypothesis probability than π. From the figure 2, it showed that the K ID requrement does not affect the efficiency for $K^{*0}K^+$ too much.

B. $f_0\pi$ tagging mode checking

The $f_0\pi$ mode is a rather difficult one. Considering the other tagging modes selection, a rather similar selection is used here. Figure 3(a) is the $f_0\pi$ mass plot by requiring that the 1-c (beam energy constraint) fit probability be greater than 10%. Figure 3(b) is the result by further requiring $|M(\pi\pi)-0.98| < 0.03\mathrm{MeV}/c^2$. Figure 3(c) is the result by further requiring the π candidate tracks have greater π hypothesis probability than K hypothesis probability. Figure 3(d)(e)(f)(g)and(h) are the results by further requiring the D_s production angle $|cos(\theta)|$ <0.9, 0.8, 0.7, 0.6 and 0.5 respectively. The $|cos(\theta)|$ <0.6 is used for $f_0\pi$ tagging.

III. ELECTRON ID

The dE/dx, TOF, and Barrel Shower Counter information is used to calculate joint confidence levels for each particle hypothesis. In order to get a high electron ID efficiency and a low hadron misidentification rate, we require the confidence level for the electron hypothesis to be above 1%, and the confidence level for the pion and kaon hypothesis to be below 5%.

Radiative Bhabha events in the same dataset are used to measure the electron ID efficiency P_{ee}, and pions from kinematicaly selected $J/\psi \to \omega\pi\pi$ events are used to estimate the hadron misidentification probability $P_{\pi e}$. The dependence of P_{ee} and $P_{\pi e}$ on particle momentum is shown in Figure 4. The P_{ee} values are weighted by the electron momentum distribution of Monte Carlo simulated $D_s^+ \to e^+X$ decays to obtain an average value of 82.4%. Similarly, the $P_{\pi e}$ distribution is weighted with the momentum distribution of pions to yield an average of 0.8%.

IV. EVENT SELECTION AND BACKGROUND SUBTRACTION

The recoil system of the single tag D_s events are searched for a well identified electron track. Recoil electrons are required to have a momentum larger than 0.2 GeV/c. This cut reduces the number of electrons from photon conversion ($\gamma \to e^+e^-$). To ensure good tracking and particle ID information, tracks have to be within the fiducial volume of $|\cos\theta| <$

0.75 and they must have a good helix fit. In addition, a cut on the angle to the nearest, oppositely charged electron track, $\cos\theta_{ee} < 0.98$, is imposed to further reduce background from gamma conversion. Figure 5 shows the $\cos\theta_{ee}$ distribution of Monte Carlo simulated e^+e^- pairs from gamma conversion, and the same distibution for the single tag sample.

In orger to exclude possible background from D_s purely leptonic decay, that is $D_s \to \tau\nu \to e\nu\nu\nu$, it is requested that at least one additional neutral or charged track exists in the recoil of D_s tag besides inclusive electron. If the electron's charge is opposite to the tag's charge, the electron is called Right Sign (RS). Otherwise, it is called Wrong Sign (WS). WS electrons are due to gamma conversion electrons and electrons from neutral pion dalitz decays which pass the momentum and opening angle cuts. This background is charge symmetric and estimated by the number of WS electrons. Figure 6 shows the single tag mass spectra when (a) a RS electron is detected in the recoil system, and (b) a WS electron is detected in the recoil system. The RS electron signal contains $D_s^+ \to e^+X$ events, as well as $D \to eX$ background, hadrons misidentified as electrons, and the charge symmetric background from surviving gamma conversions and π^0 Dalitz decays. The number of hadrons misidentified as electrons can be estimated from the number of hadrons in the recoil system N_h, multiplied by the hadron mis-ID probability P_{he}. Here we approximate the misidentification probability of kaons to be equal to that of pions: $P_{he} \approx P_{\pi e} = 0.8\%$. This will cause a small systematic error, which is estimated and added to the systematic error of the branching fraction. Figure 7(a) and 7(b) shows the single tag mass spectra for RS and WS hadron tracks in the recoil system.

The corrected spectrum with charge symmetric backgrounds and hadron misidentifications subtracted is shown in Figure 8. Since the $D \to eX$ background is roughly continuous and approximately flat, the peak at 1.97 GeV/c^2 in Figure 8 is due to the D_s semileptonic decay. A simple fit using a second order polynomial and a Gaussian finds that the peak is centered at D_s.

Figures 6, 7 and 8 show the result by five D_s tagging modes. Because the single tagging signal of $f_0\pi$ is not good, figure 9 show the result of four D_s tagging mode without $f_0\pi$ decay mode.

V. MONTE CARLO SIMULATION AND EVENT SELECTION EFFICIENCY

After the single tagging, the efficiency of the event selection is merely the detecting efficiency of the electron track, which includes the fiducial cut acceptance, the momentum cut acceptance, the $\cos\theta_{ee} < 0.98$ acceptance, and the electron ID probability P_{ee}. The first three parts lead to an acceptance of 65%, which is determined by Monte Carlo simulation. The overall efficiency is 53% which takes the P_{ee} (82%) into account. The Monte Carlo simulation consists of the three major semileptonic decay modes $\phi e\nu$, $\eta e\nu$, and $\eta' e\nu$, with relative branching ratios measured by CLEO II [5]. The uncertainty of the existence of other D_s exclusive semileptonic decays only causes an error of less than 3% in the efficiency estimation.

VI. ESTIMATION OF THE BRANCHING FRACTION

The estimation of the branching fraction is based on the number of signal events in the histograms for the RS and WS electrons and hadrons, as well as the number of D_s tags. In each histogram, signal events follow a Gaussian distribution $f_1(x)$ centered at $x_0 = 1968.7 \pm 0.6$ MeV$/c^2$ with a standard deviation of $\sigma = 3.9 \pm 0.6$ MeV$/c^2$. The parameters are determined from a fit to the distribution of the single tags. In the same fit, the distribution of the background events is approximated by a quadratic function $f_2(x)$ for the combinatorial background plus a Gaussian distribution $f_3(x)$ centered at 1948.3MeV$/c^2$. All three functions are normalized to unit integral.

We set up an unbinned extended likelihood for the number of signal and background events (s, b_1 and b_2, respectively) in each histogram:

$$\mathcal{L}(s, b_1, b_2) = e^{-s-b_1-b_2} \prod_{i=1}^{N} [s f_1(x_i) + b_1 f_2(x_i) + b_2 f_3(x_i)]. \tag{1}$$

The total likelihood function is the product of the five likelihood function in the five histograms, the RS electron, WS electron, RS hadron, WS hadron and single tag. There are two ways to extract out the $Br(D_s \to eX)$, one is to use the MINUIT to minimize the likelihoodfuction, and the other is to use marginalization method.

A. Method 1: Maximization of the Likelihood Function by MINUIT

Using MINUIT, the braching fraction of $D_s \to eX$ is got as: $Br(D_s \to eX) = (7.62^{+5.49}_{-4.60})\%$ for four tagging modes, and $Br(D_s \to eX) = (8.43^{+5.02}_{-4.21})\%$ for five tagging modes including the $f_0\pi^+$ mode.

B. Method 2: Marginalization of the Likelihood Function

To obtain a likelihood for the number of signal events alone, we marginalize $\mathcal{L}(s, b_1, b_2)$ with respect to b_1 and b_2:

$$\mathcal{L}(s) = \int_0^\infty \int_{-\infty}^\infty \mathcal{L}(s, b_1, b_2)\, db_2\, db_1. \tag{2}$$

For both the electrons and the hadrons, we calculate the likelihood for the net number $N_{net} = N_{RS} - N_{WS}$ as a product of the two likelihoods $\mathcal{L}_{RS}(N_{RS})$ and $\mathcal{L}_{WS}(N_{WS})$ and marginalize it:

$$\mathcal{L}(N_{net}) = \int_{-\infty}^\infty \mathcal{L}_{RS}(N_{RS}) \mathcal{L}_{WS}(N_{RS} - N_{net})\, dN_{RS}. \tag{3}$$

Using the values for the particle identification probabilities, we correct the net number of electrons and obtain a likelihood for the true number of electrons, $N^e_{true} = (N^e_{net} - P_{he} N^h_{net})/P_{ee}$, and marginalize with respect to the number of hadrons. Finally, we calculate the branching fraction

$$Br(D_s \to e\nu X) = \frac{N^e_{true}}{\varepsilon_{geom} N_{tag}}. \tag{4}$$

Figure 10 shows the resulting likelihood as a function of the branching fraction. The shaded area on the left (right) corresponds to 31.73 % of the area under the curve on the left (right) side of the maximum. The unshaded region is the error interval.

This method leads to the result of $Br(D_s \to eX) = (6.30^{+6.07}_{-4.47})\%$ for four tagging modes, and $Br(D_s \to eX) = (7.74^{+5.73}_{-4.35})\%$ for five tagging modes including $f_0\pi$ mode.

The systematic error is mainly estimated on the basis of the changes of $Br(D_s \to e\ X)$ due to variations in the electron momentum cut ($\pm 1.9\%$), the shape of the background ($\pm 0.5\%$), the electron detection efficiency ($^{+0.5}_{-0.1}\%$), the hadron misidentification rate ($^{+0.9}_{-0.7}\%$), the width of the bump around 1.948 GeV/c^2 ($^{+0.4}_{-0.1}\%$) and the geometric efficiency ($^{+0.6}_{-0.2}\%$). The combined effect of these sources is obtained by adding in the uncertainties in quadrature, which yeilds a total systematic error of ($^{+2.4}_{-2.1}\%$).

VII. CONCLUSION

Our measurement is consistent with the MARK-III [3] measurement, but has smaller errors. Considering the lifetimes of the charmed mesons given by PDG, our branching fraction corresponds to a D_s semileptonic decay width of $\Gamma(D_s^+ \to e^+X) = (1.32^{+1.41+0.51}_{-1.02-0.45}) \times 10^{11}s^{-1}$, while MARK-III's measurements [2] lead to $\Gamma(D^+ \to e^+X) = (1.63 \pm 0.18) \times 10^{11}s^{-1}$ and $\Gamma(D^0 \to e^+X) = (1.86 \pm 0.29) \times 10^{11}s^{-1}$. Comparison of these decay widths shows that semileptonic decays of charmed mesons are consistent with the description of the spectator model, $\Gamma_{SL}(D^+) = \Gamma_{SL}(D^0) = \Gamma_{SL}(D_s^+)$.

REFERENCES

* Present address: Kansas State University, Manhattan, Kansas.

** Present address: Stanford Linear Accelerator Center, Stanford, California 94309.

† Work supported in part by the National Natural Science Foundation of China under Contract No. 19290400 and the Chinese Academy of Sciences under contract No. KJ85 (IHEP); by the Department of Energy under Contract Nos. DE-FG02-91ER40676 (Boston University), DE-FG03-92ER40701 (Caltech), DE-FG03-93ER40788 (Colorado State University), DE-AC02-76ER03069 (MIT), DE-AC03-76SF00515 (SLAC), DE-FG03-91ER40679 (UC Irvine), DE-FG03-94ER40833 (U Hawaii), DE-FG05-92ER40736 (UT Dallas), DE-AC35-89ER40486 (SSC Lab); by the U.S. National Science Foundation, Grant No. PHY9203212 (University of Washington); and by the Texas National Research Laboratory Commission under Contract Nos. RGFY91B5, RGFY92B5 (Colorado State), and RCFY93-316H (UT Dallas).

[1] PDG, Phys. Rev. D50(1994)

[2] Baltrusaitis, *et al.*, Phys. Rev. Lett. 54(1985)1976.

[3] Bai *et al.*, Phys. Rev. Lett. 65(1990)686.

[4] J.Z.Bai, *et al.*, Nucl. Instr. Meth., A344(1994)319.

[5] G. Brandernburg *et al.*, preprint CLNS 95-1351.

FIGURES

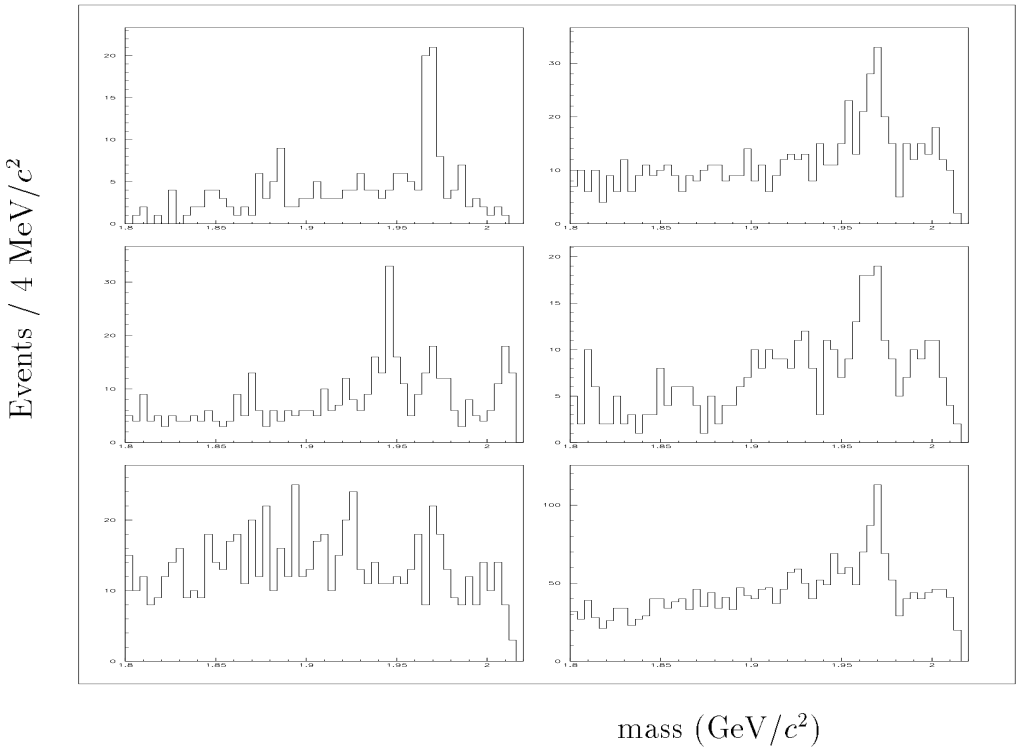

FIG. 1. Invariant mass distribution of D_s single tags calculating using the 1-C kinematic fit: (a) $\phi\pi^+$; (b) $\bar{K}^{*0}K^+$; (c) $K_S^0K^+$; (d) $K_S^0K^-\pi^+\pi^+$; (e) $f_0\pi^+$; and (f) combined.

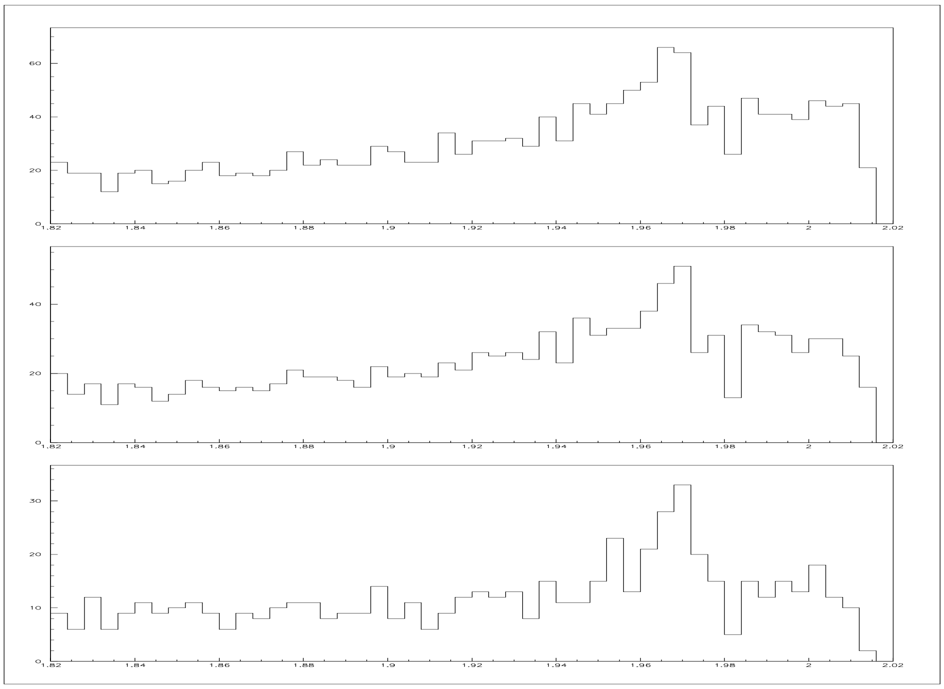

FIG. 2. K*K tag.

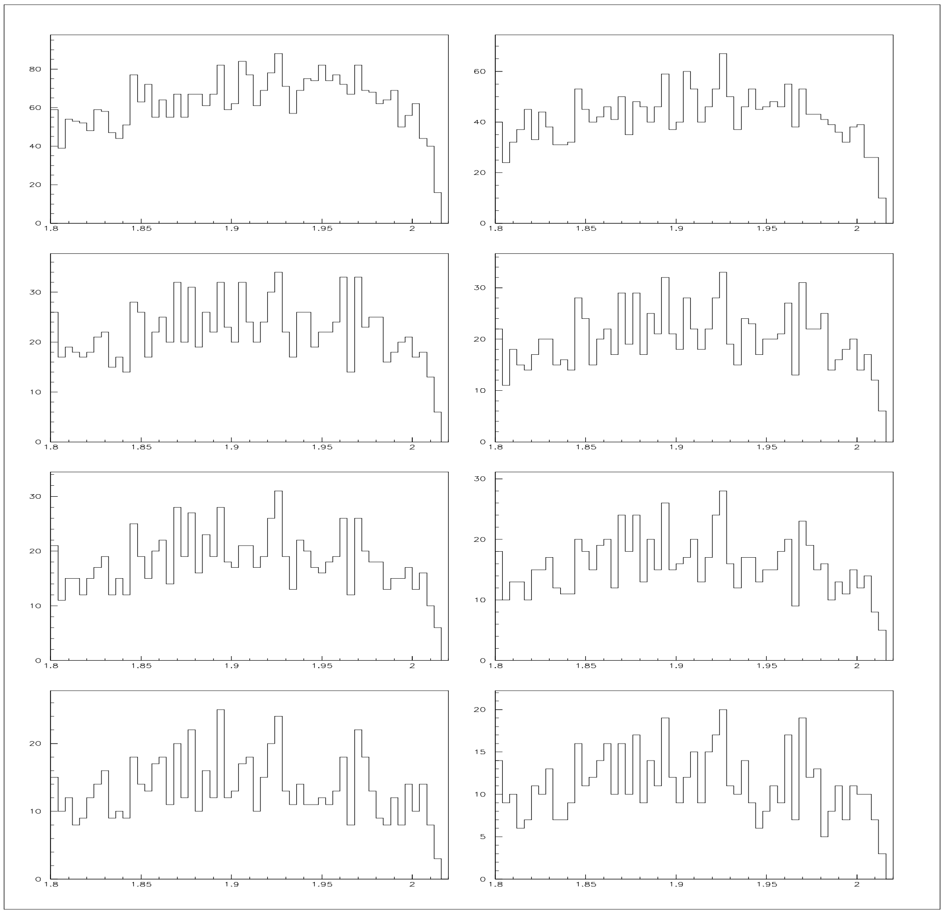

FIG. 3. f0pi tag.

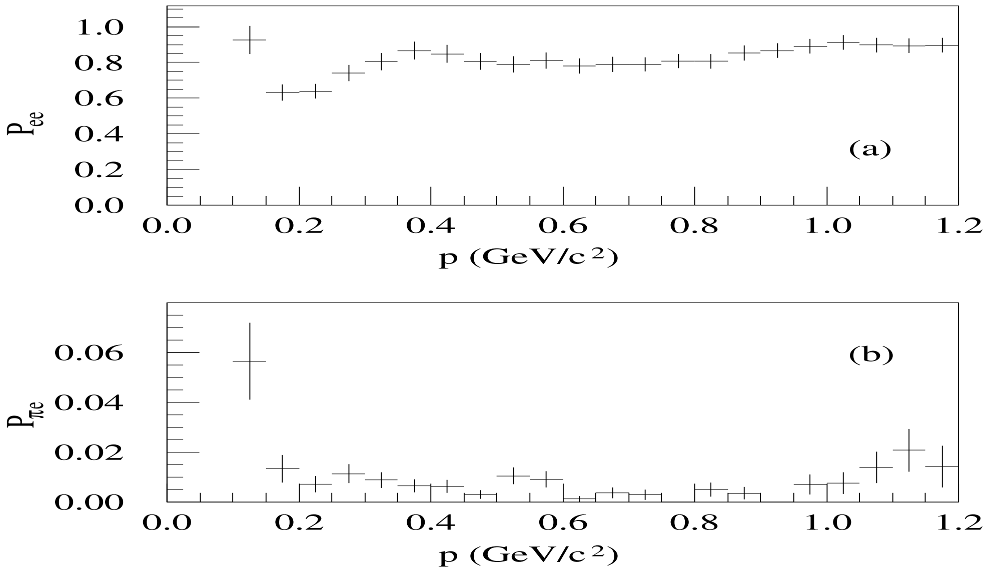

FIG. 4. Electron ID effeciency and mis-ID rate.

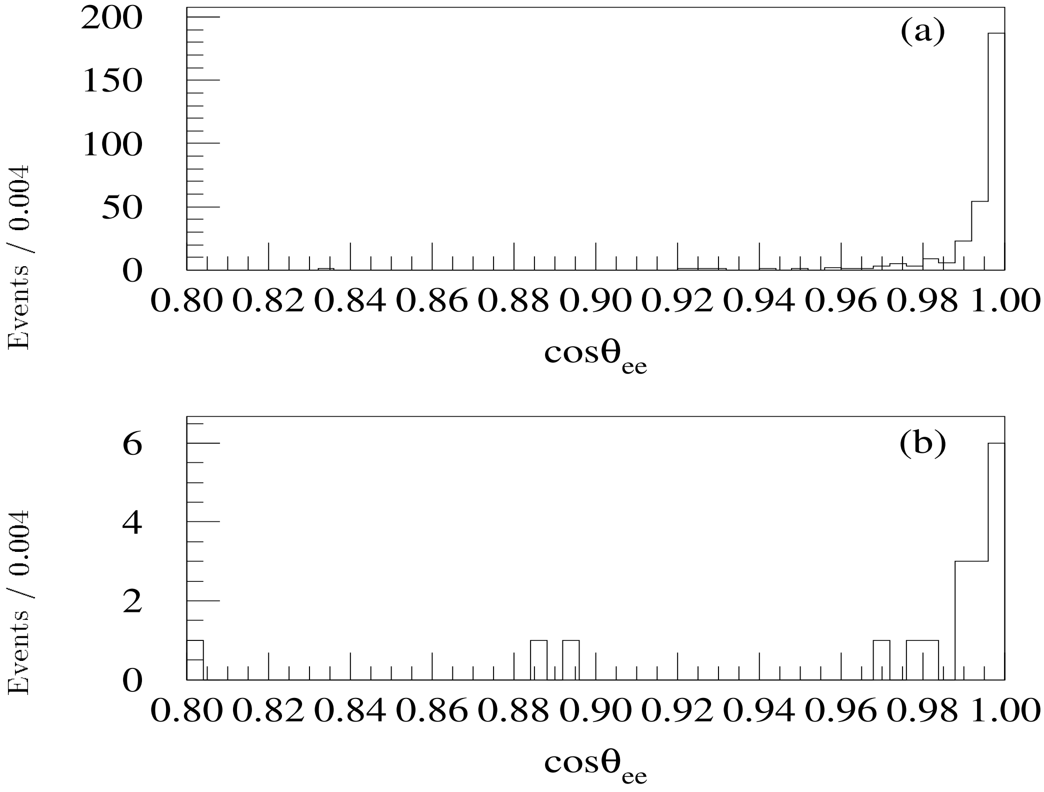

FIG. 5. Distribution of $\cos\theta_{ee}$ in (a) M.C. simulated gamma conversion events; (b) recoil tracks of the single tag sample.

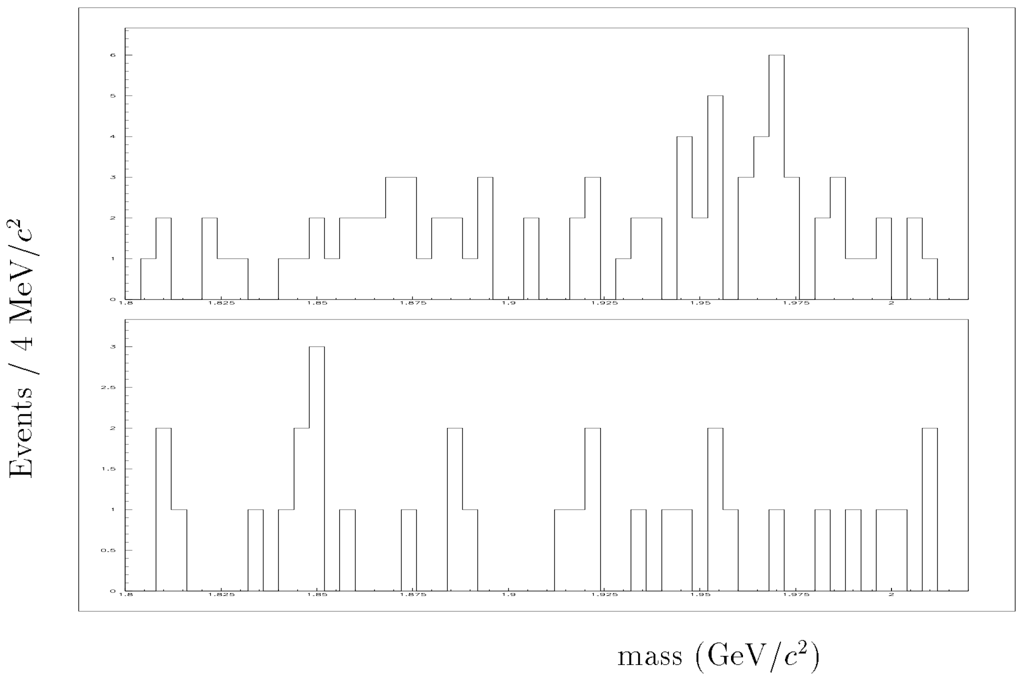

FIG. 6. Single tag mass spectra when (a) a RS electron or (b) a WS electron is detected in the recoil system.

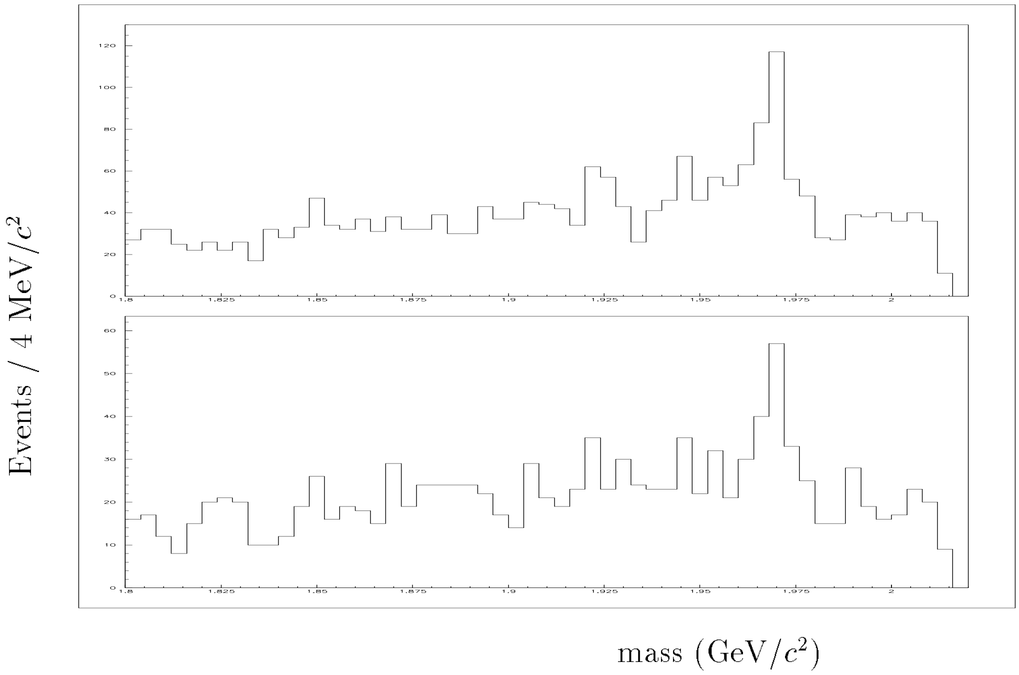

FIG. 7. Single tag mass spectra for (a) RS hadron tracks, and (b) WS hadron tracks in the recoil system.

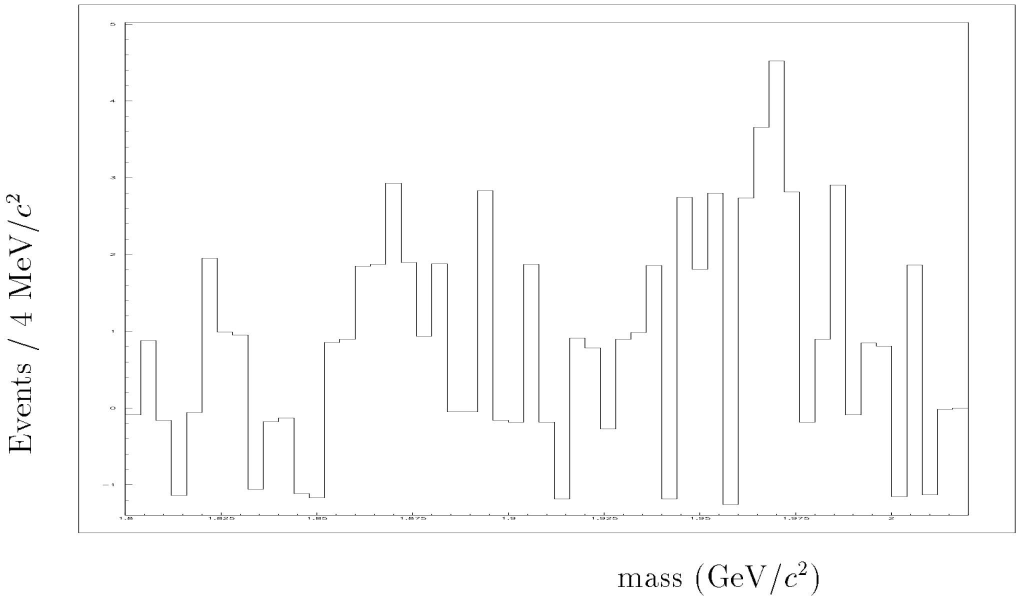

FIG. 8. Single tag mass spectrum of RS-WS electrons corrected for hadron misidenification.

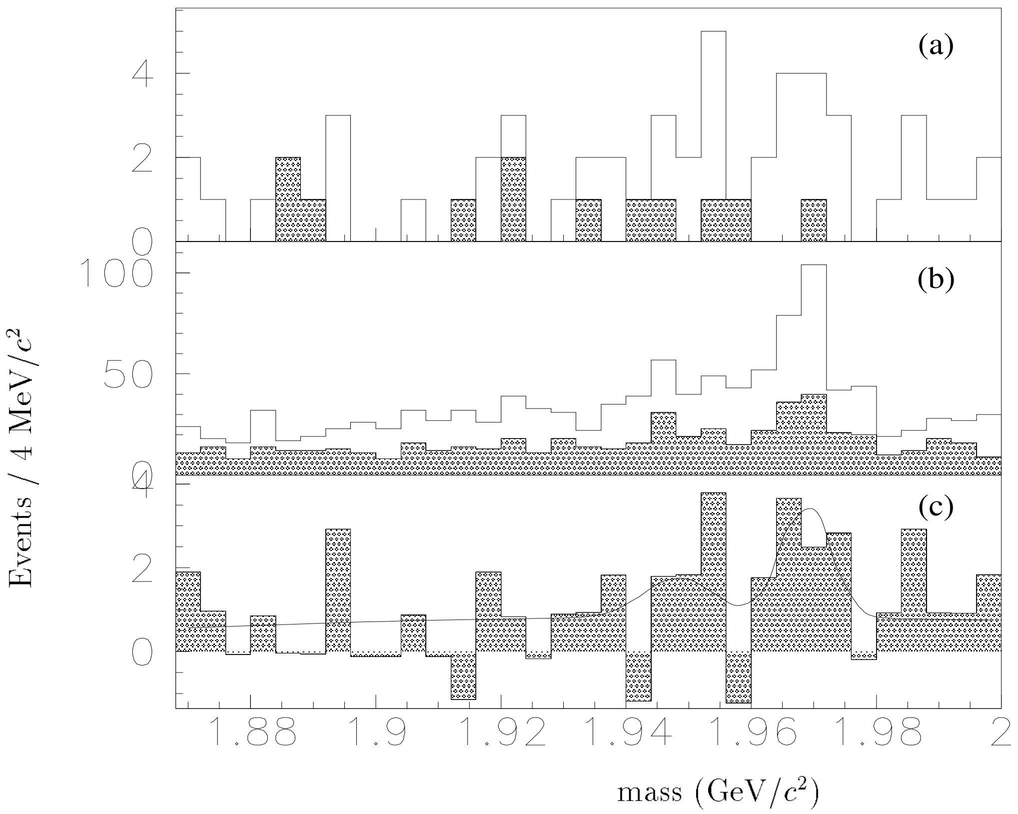

FIG. 9. (a) Single tag mass spectra when a RS (unshaded) and a WS electron (shaded) is detected in the recoil system. (b) Single tag mass spectra when a RS (unshaded) and a WS hadron (shaded) is detected in the recoil system. (c) Single tag mass spectrum of RS-WS electrons corrected for hadron misidenification.

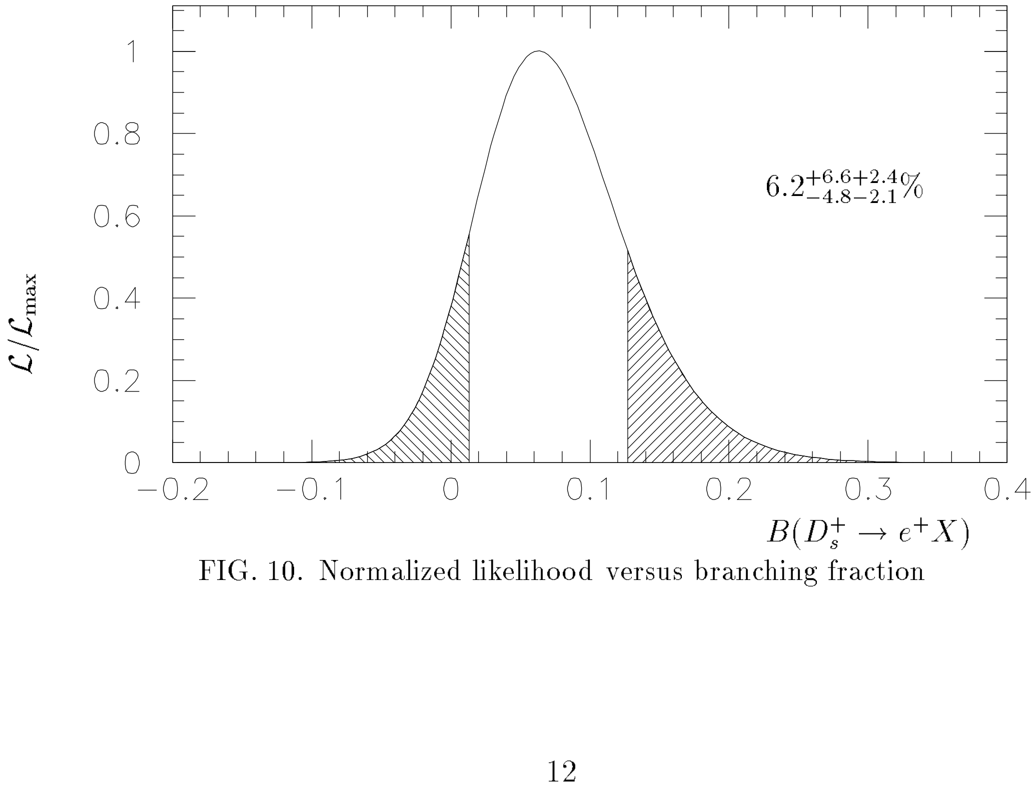

FIG. 10. Normalized likelihood versus branching fraction